

Comparison of Structural Subscapularis Integrity After Latarjet Procedure Versus Iliac Crest Bone Graft Transfer

Paul Siegert,^{*†} MD, Fabian Plachel,[†] MD, PhD, Doruk Akgün,[†] MD, Alexander D.J. Baur,[‡] MD, Eva Schulz,[§] MD, Alexander Auffarth,[§] MD, Mark Tauber,^{||} MD, and Philipp Moroder,[†] MD

Investigations performed at the Department for Shoulder and Elbow Surgery, Charité–Universitätsmedizin Berlin, Center for Musculoskeletal Surgery, Berlin, Germany

Background: Although clinical outcome scores are comparable after coracoid transfer procedure (Latarjet) and iliac crest bone graft transfer (ICBGT) for anterior shoulder instability with glenoid bone loss, a significant decrease in internal rotation capacity has been reported for the Latarjet procedure.

Hypothesis: The subscapularis (SSC) musculotendinous integrity will be less compromised by ICBGT than by the Latarjet procedure.

Study Design: Cohort study; Level of evidence, 3.

Methods: We retrospectively analyzed pre- and postoperative computed tomography (CT) scans at short-term follow-up of 52 patients (26 Latarjet, 26 ICBGT) previously assessed in a prospective randomized controlled trial. Measurements included the preoperative glenoid defect area and graft area protruding the glenoid rim at follow-up and tendon thickness assessed through SSC and infraspinatus (ISP) ratios. Fatty muscle infiltration was graded according to Goutallier, quantified with muscle attenuation in Hounsfield units, and additionally calculated as percentages. We measured 3 angles to describe rerouting of the SSC musculotendinous unit around the bone grafts.

Results: SSC fatty muscle infiltration was $2.0\% \pm 2.2\%$ in the Latarjet group versus $2.4\% \pm 2.2\%$ in ICBGT ($P = .546$) preoperatively and showed significantly higher values in the Latarjet group at follow-up ($5.3\% \pm 4.5\%$ vs $2.3\% \pm 1.7\%$; $P = .001$). In total, 4 patients (15.4%) in the Latarjet group showed a progression from grade 0 to grade 1 at follow-up, whereas no changes in the ICBGT group were noted. The measured rerouting angle of the SSC muscle was significantly increased in the Latarjet group ($11.8^\circ \pm 2.1^\circ$) compared with ICBGT ($7.5^\circ \pm 1.3^\circ$; $P < .001$) at follow-up, with a significant positive correlation between this angle and fatty muscle infiltration ($R = 0.447$; $P = .008$). Ratios of SSC/ISP tendon thickness were 1.03 ± 0.3 in the Latarjet group versus 0.97 ± 0.3 ($P = .383$) in ICBGT preoperatively and showed significantly lower ratios in the Latarjet group (0.7 ± 0.3 vs 1.0 ± 0.2 ; $P < .001$) at follow-up.

Conclusion: Although clinical outcome scores after anterior shoulder stabilization with a Latarjet procedure and ICBGT are comparable, this study shows that the described decline in internal rotation capacity after Latarjet procedure has a radiographic structural correlate in terms of marked thinning and rerouting of the SSC tendon as well as slight fatty degeneration of the muscle.

Keywords: Latarjet; iliac crest bone graft transfer; subscapularis; shoulder instability

Glenoid bone augmentation procedures have shown to be superior to mere soft tissue stabilization for treatment of anterior shoulder instability with extensive glenoid bone loss.^{5,6} To restore glenoid bone integrity, various grafting procedures have been established. However, coracoid and free bone transfer are distinguished as the 2 main surgical approaches.^{1,3,14,16,25} The current study provides a comparative analysis of iliac crest bone graft transfer (ICBGT) in

terms of the implant free J-bone graft technique³ and the Latarjet procedure.²⁵ To reconstitute the glenoid rim, in the ICBGT, a J-shaped bone graft, harvested from the iliac crest, is press-fit into an osteotomy at the anterior glenoid neck (Figure 1). In the Latarjet procedure, the coracoid process, along with the conjoint tendons, is used as a bone graft and implanted onto the anterior glenoid neck through screw fixation.¹⁶ Although the ICBGT requires a temporary, horizontal split of the subscapularis (SSC), the Latarjet procedure redirects the conjoint tendon through a permanent SSC split to enhance anterior shoulder stability via an additional sling effect.¹¹

The Orthopaedic Journal of Sports Medicine, 8(10), 2325967120958007

DOI: 10.1177/2325967120958007

© The Author(s) 2020

This open-access article is published and distributed under the Creative Commons Attribution - NonCommercial - No Derivatives License (<https://creativecommons.org/licenses/by-nc-nd/4.0/>), which permits the noncommercial use, distribution, and reproduction of the article in any medium, provided the original author and source are credited. You may not alter, transform, or build upon this article without the permission of the Author(s). For article reuse guidelines, please visit SAGE's website at <http://www.sagepub.com/journals-permissions>.

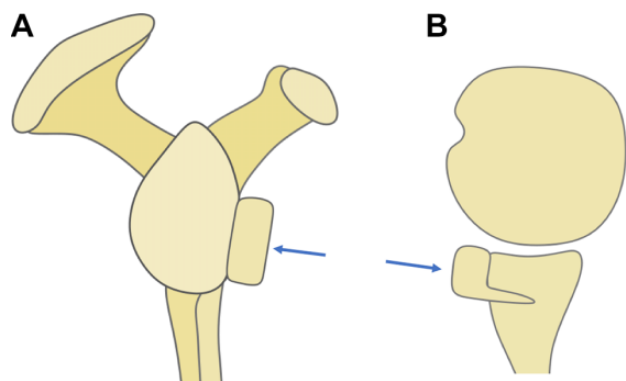


Figure 1. Schematic illustration of an iliac crest J-bone graft (blue arrow) inserted into an osteotomy at the anterior glenoid neck with press-fit fixation on (A) en face and (B) axial views.

A recent prospective, randomized controlled study²⁰ analyzing these 2 procedures for anterior shoulder instability showed no differences regarding main outcome measures at short-term follow-up but observed a significant postoperative decrease of internal rotation with the arm adducted and held at 90° of abduction in patients after Latarjet procedure compared with ICBGT. This effect is thought to be the result of a mechanical influence of the conjoint tendons and screw fixation on structural SSC muscle integrity and redirection of the musculotendinous unit around the graft.²⁰

The aim of this study was to identify the influence of glenoid bone augmentation with Latarjet procedure versus ICBGT on integrity and rerouting of the SSC musculotendinous unit. We hypothesized that the integrity of the SSC tendon and muscle is less compromised after ICBGT compared with the Latarjet procedure.

METHODS

Approval from the regional ethics committees was obtained before onset of the investigation.

Study Population

For this retrospective evaluation of prospectively acquired data, we enrolled 60 eligible patients who underwent either the Latarjet (n = 30) procedure or ICBGT (n = 30) for

anterior shoulder instability with critical bone loss within the recruitment period between 2012 and 2015 and had been previously assessed in a prospective randomized controlled trial.²⁰ In the prior study, inclusion criteria were (1) anterior shoulder instability with ≥ 2 recurrent dislocations and (2) glenoid bone loss $\geq 15\%$ of the glenoid articular surface measured with the PICO method.⁴ Exclusion criteria included (1) any concomitant shoulder pathologies (eg, cuff tears, nerve lesions, osteoarthritis $> 1^\circ$); (2) previous surgeries of the affected shoulder other than open or arthroscopic Bankart repairs; (3) neuromuscular pathologies including seizure disorders; (4) previous history of infection; (5) compliance problems (eg, alcohol or drug abuse); and (6) unwillingness to participate in the study.

Of this cohort, all patients with (1) lack of follow-up CT scans (minimum 12 months after surgery) and (2) CT scans not covering the medial border of the scapula and at least 75% of the craniocaudal scapular extent were excluded from the current study.⁸

After application of these criteria, the final cohort included 26 patients receiving ICBGT with a mean \pm SD follow-up of 24.5 ± 3.2 months and 26 patients with Latarjet procedure with a mean follow-up of 21.7 ± 6.8 months ($P = .120$). The Latarjet group included 1 female and 25 male patients with a mean age of 29.6 years (range, 20-57 years) and the ICBGT group included 1 female and 25 male patients with a mean age of 31.8 years (range, 16-47 years; $P = .386$) at the time of surgery.

Interventions

Detailed descriptions of the randomization process as well as surgical procedures for ICBGT and Latarjet were provided in a previous publication.²⁰

Radiographic Assessment

For preoperative and follow-up evaluation, patients underwent CT examination with a primary slice thickness of 0.625 mm. All multiplanar reconstructions and measurements were independently conducted by 2 observers (P.S., F.P.) using Visage 7.1 (Visage Imaging) software.

Glenoid Measurements

Preoperatively, glenoid defects were measured using the PICO method on en face views.⁴ The defect area of the

*Address correspondence to Paul Siegert, MD, Charité–Universitätsmedizin Berlin, Corporate Member of Freie Universität Berlin, Humboldt-Universität zu Berlin, and Berlin Institute of Health, Center for Musculoskeletal Surgery, Department for Shoulder and Elbow Surgery, Berlin 13353, Germany (email: paul.siegert@charite.de).

[†]Charité–Universitätsmedizin Berlin, Corporate Member of Freie Universität Berlin, Humboldt-Universität zu Berlin, and Berlin Institute of Health, Center for Musculoskeletal Surgery, Department for Shoulder and Elbow Surgery, Berlin, Germany.

[‡]Charité–Universitätsmedizin Berlin, Corporate Member of Freie Universität Berlin, Humboldt-Universität zu Berlin, and Berlin Institute of Health, Department of Radiology, Berlin, Germany.

[§]Department of Orthopedics and Traumatology, Paracelsus Medical University, Salzburg, Austria.

^{||}Department for Shoulder and Elbow Surgery, ATOS Clinic Munich, Munich, Germany.

Final revision submitted July 8, 2020; accepted July 29, 2020.

The authors declared that there are no conflicts of interest in the authorship and publication of this contribution. AOSSM checks author disclosures against the Open Payments Database (OPD). AOSSM has not conducted an independent investigation on the OPD and disclaims any liability or responsibility relating thereto.

Ethical approval for this study was obtained from the regional ethics committee for Salzburg Austria, and the ATOS-Klinik ethics committee.

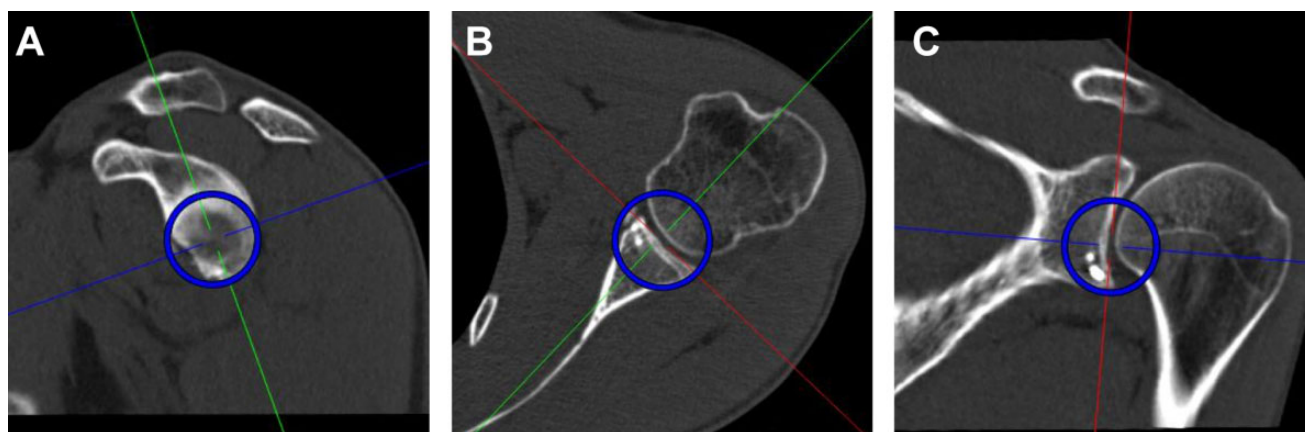


Figure 2. A spherical volume of interest (blue circles) was set on (A) an en face view as a best-fit circle, with its center at the deepest point of the glenoid concavity, which allowed measurements on the (B) transverse and (C) coronal planes.

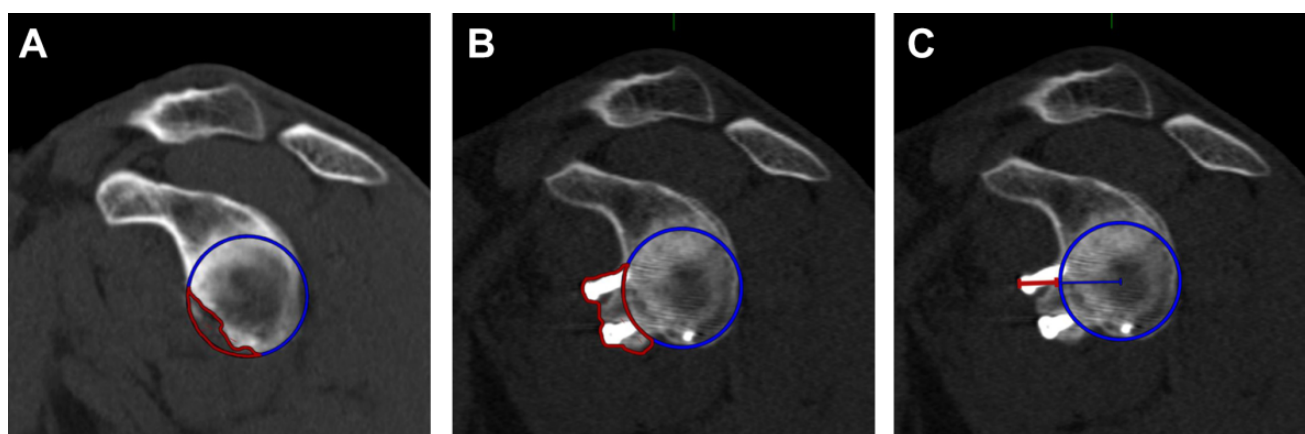


Figure 3. (A) Preoperative glenoid defect measured with the PICO method on an en face view. (B) Area protruding (red) the best-fit circle (blue) at latest follow-up, calculated as percentage in respect to the best-fit circle area. (C) Widest diameter protruding the best-fit circle, measured from the center of the glenoid in millimeters.

glenoid was calculated as a percentage of the best-fit circle area. For later measurements, the best-fit circle on an en face view was constituted as a spherical volume of interest (VOI) with its center defined at the midpoint of the glenoid concavity to allow measurements of the former glenoid rim on the transverse plane (Figure 2). At follow-up, a spherical VOI with the same diameter as preoperatively was drawn on an en face view of the glenoid, and the graft area (including screws) protruding the best-fit circle was measured and calculated as a percentage in respect to the best-fit circle area. Additionally, widest expansion of the graft diameter measured from the center of the glenoid protruding the best-fit circle was measured in millimeters (Figure 3).

SSC Route

For the measurement of the SSC route around the grafts, 3 different angles were measured. To determine SSC routing around the native (preoperative) glenoid, we measured an

angle between a line from the medial border of the scapula to the center of the glenoid (defined by the center of the spherical VOI) and a line from the medial border of the scapula to the most anterior extent of the glenoid rim on the transverse plane. At follow-up, the same angle was measured to the extent of the most anterior aspect of the respective graft. To define the theoretically physiologic SSC route (glenoid without bone defect), we measured the angle between a line from the medial border of the scapula to the center of the glenoid and a tangent line from the medial border of the scapula to the spherical VOI (Figure 4). Measurements of SSC routes were referenced to only the anatomic features of the scapula to prevent the influence of varying humeral head translation.

SSC Musculotendinous Integrity

To measure atrophy or thinning of the SSC musculotendinous interface, a tangent to the surface of the glenoid was

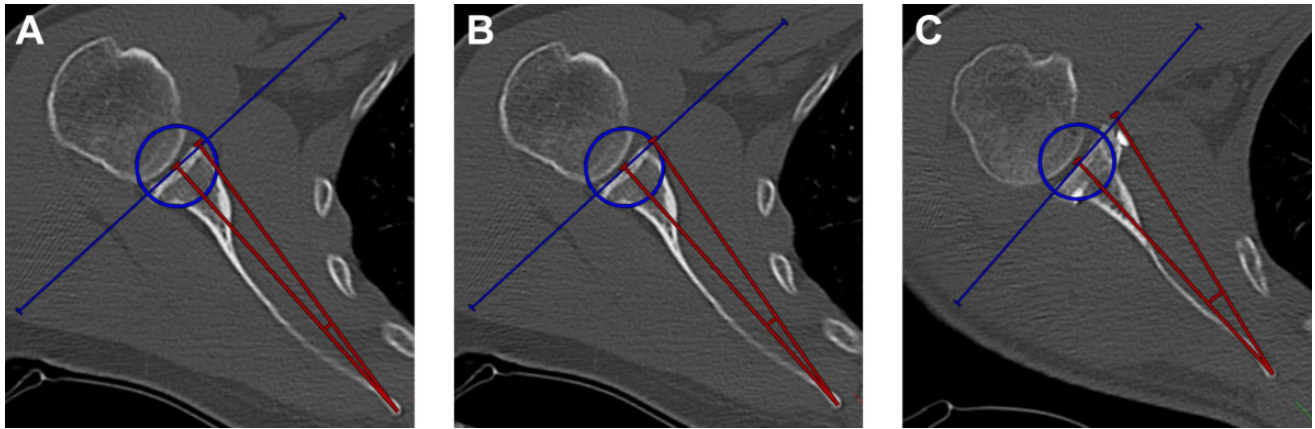


Figure 4. Subscapularis routing angles (red) are measured between the line from the medial scapular ridge to the center of the glenoid and the line from the medial scapular ridge to the (A) preoperative, native, most anterior border of the glenoid, (B) interception of a glenoid tangent and the best-fit circle, and (C) most anterior extent of the respective graft.

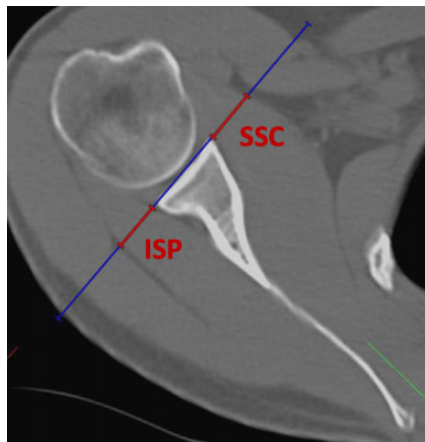


Figure 5. Measurement of subscapularis (SSC) and infraspinatus (ISP) tendon thicknesses on the transverse plane at the level of the glenoid center. A ratio of SSC tendon thickness divided by ISP tendon thickness was calculated.

drawn at the level of the glenoid center on the transverse plane, and the respective thicknesses of the SSC and infraspinatus (ISP) tendons were measured on this tangent as proposed by Maynou et al.¹⁷ Ratios were calculated by dividing tendon thicknesses in millimeters of SSC through ISP (Figure 5).

SSC Muscle Atrophy and Fatty Infiltration

SSC muscle integrity was measured on a parasagittal image plane at the most lateral image on which the coracoid process and the spine of the scapula form a Y-shape.²¹ A vertical diameter, an upper transverse diameter (UTD) at the concavity of the scapular body, and a lower transverse diameter (LTD) at the most inferior aspect of the scapular body were measured in millimeters (Figure 6A).^{21,22,24}

Fatty infiltration of the SSC muscles was graded on the parasagittal (Y-) image plane via the Goutallier

classification, with grade 0 being normal muscle; grade 1, muscle with fatty streaks; grade 2, muscle content greater than fat content; grade 3, muscle and fat equal; and grade 4, muscle content less than fat content.¹³ Additionally, a region of interest (ROI) was drawn around the SSC muscle on a single representative slice, and the mean muscle attenuation was measured in Hounsfield units (HU) (Figure 6C). The teres minor (TM) and ISP were measured together, because exact separation of these 2 muscles is not feasible.²⁶ To portray upper muscle attenuation (UMA) and lower muscle attenuation (LMA) of the SSC, 2 circular ROIs with a circumference of 25 mm were drawn at the level of the UTD and the LTD (Figure 6B).²⁴ For quantitative measurements, DICOM data from images on the parasagittal (Y-) image plane were exported and analyzed using ImageJ software (National Institutes of Health).²³ According to Aubrey et al,² the threshold for adipose tissue was set to -190 to -30 HU. A ROI was drawn around the SSC and ISP/TM muscles. Voxels within the defined -190 and -30 HU (adipose tissue) were extracted and calculated as percentages from the respective ROI (Figure 7).

Statistics

For statistical analyses, we used SPSS Statistics Version 24.0 (IBM) software. $P < .05$ was considered significant. Descriptive statistics, including mean, standard deviation, and minimum and maximum values of continuous variables, were calculated. Two raters (P.S. and F.P.) conducted the measurements independently at different time points. An intraclass correlation coefficient (ICC) with 95% CI was calculated for all measurements. As recommended by Landis and Koch,¹⁵ an ICC < 0.20 is considered slight agreement, 0.21 to 0.40 fair agreement, 0.41 to 0.60 moderate agreement, 0.61 to 0.80 substantial agreement, and > 0.81 almost perfect agreement.¹⁵ After reliability assessment, values of both raters were averaged for further analysis. Statistical differences

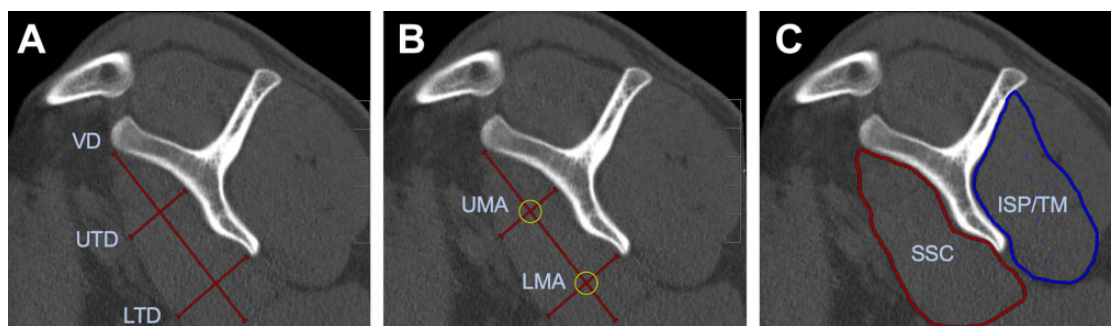


Figure 6. (A) Measurement of subscapularis (SSC) muscle diameters. LTD, lower transverse diameter; UTD, upper transverse diameter; VD, vertical diameter. (B) Measurement of muscle attenuation in Hounsfield units (HU) of upper muscle attenuation (UMA) and lower muscle attenuation (LMA) of SSC muscle. (C) Mean muscle attenuation in HU of SSC and infraspinatus/teres minor (ISP/TM) muscles.

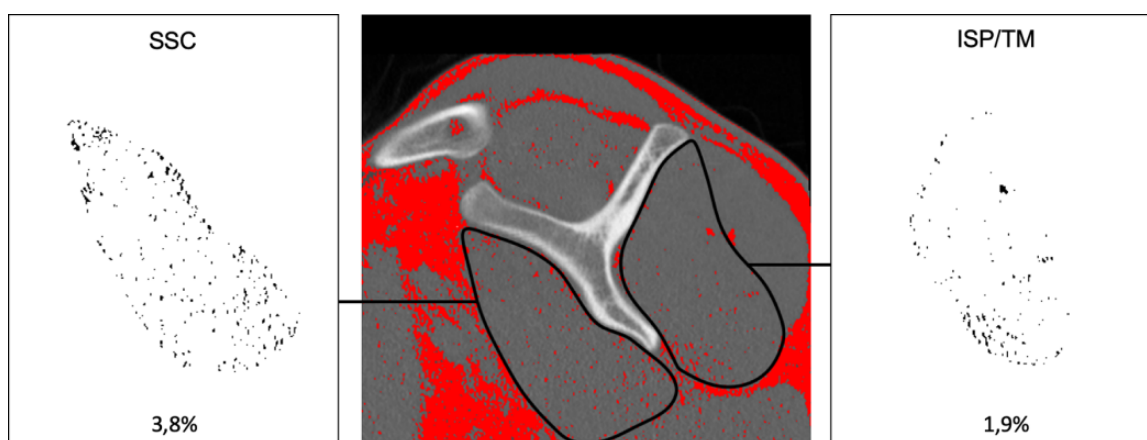


Figure 7. Voxel-based quantification of fatty infiltration of subscapularis (SSC) and infraspinatus/teres minor (ISP/TM) muscles. The threshold for adipose tissue was set at -190 to -30 Hounsfield units (red). Areas of respective muscles were marked, and fatty infiltration was calculated as percentage of the muscle area.

between measurements were determined by independent *t* test. To analyze correlations between parameters, the Pearson correlation coefficient was determined. A linear regression model was calculated to investigate the influence of graft parameters on fatty infiltration of the SSC muscle.

RESULTS

All measurements showed substantial to almost perfect agreement between the 2 raters. The ICCs are summarized in Table 1.

Glenoid Measurements

The mean preoperative glenoid defect was $18.2\% \pm 2.4\%$ and $18.0\% \pm 2.0\%$ in the Latarjet and ICBGT groups ($P = .704$), respectively. At follow-up, the measured graft area protruding the best-fit circle was $15.2\% \pm 8.2\%$ in the Latarjet group compared with $1.5\% \pm 2.0\%$ ($P < .001$)

in ICBGT, and the widest graft overhang was significantly larger in the Latarjet group (7.0 ± 2.6 vs 1.0 ± 1.0 mm; $P < .001$).

SSC Route

Although preoperative routing angles ($5.7^\circ \pm 0.7^\circ$ vs $5.5^\circ \pm 0.7^\circ$; $P = .338$) and physiologic routing ($7.5^\circ \pm 0.4^\circ$ vs $7.5^\circ \pm 0.3^\circ$; $P = .627$) in Latarjet and ICBGT, respectively, were comparable, we observed a significantly larger mean rerouting angle in the Latarjet group ($11.8^\circ \pm 2.1^\circ$) compared with ICBGT ($7.5^\circ \pm 1.3^\circ$; $P < .001$) at follow-up.

SSC Musculotendinous Integrity

Ratios of SSC/ISP tendon thickness were 1.03 ± 0.3 in the Latarjet group versus 0.97 ± 0.3 ($P = .383$) in ICBGT preoperatively, but the Latarjet group had significantly lower ratios at follow-up (0.70 ± 0.3 vs 1.00 ± 0.2 ; $P < .001$) (Figure 8).

TABLE 1
Calculated Intraclass Correlation Coefficients (ICC) for All Measurement Parameters With 95% CIs^a

	ICC	95% CI		Agreement
		Lower Bound	Upper Bound	
Glenoid defect	0.731	0.573	0.836	Substantial
Graft area over best-fit circle	0.929	0.880	0.959	Almost perfect
Graft width over best-fit circle	0.895	0.824	0.939	Almost perfect
Ratios of SSC/ISP tendon thickness	0.856	0.795	0.900	Almost perfect
SSC routing angles	0.959	0.945	0.970	Almost perfect
Attenuation SSC/ISP/TM	0.969	0.959	0.976	Almost perfect
Attenuation upper/lower SSC	0.990	0.987	0.992	Almost perfect
Fatty infiltration SSC/ISP/TM	0.975	0.968	0.981	Almost perfect
Goutallier classification SSC/ISP/TM	1.000	1.000	1.000	Almost perfect
SSC diameter	0.986	0.987	0.992	Almost perfect

^aISP, infraspinatus; SSC, subscapularis; TM, teres minor.

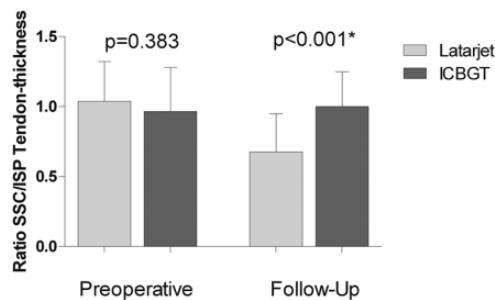


Figure 8. Mean ratios with SDs of tendon thicknesses (subscapularis [SSC]/infraspinatus [ISP]) for both groups preoperatively and at last follow-up. ICBGT, iliac crest bone graft transfer. *Significant difference.

SSC Muscle Atrophy and Fatty Infiltration

Although 4 patients (15.4%) in the Latarjet group showed a progression from Goutallier grade 0 to grade 1 at follow-up, there was no change in ICBGT. Neither group had a significant decrease in mean UMA and LMA. SSC fatty muscle infiltration was $2.0\% \pm 2.2\%$ in the Latarjet group versus $2.4\% \pm 2.2\%$ in ICBGT ($P = .546$) preoperatively and showed slightly but significantly higher values in the Latarjet group at follow-up ($5.3\% \pm 4.5\%$ vs $2.3\% \pm 1.7\%$; $P = .001$) (Table 2).

Influence of Graft Parameters on SSC Muscle Integrity

A linear regression model ($R = 0.447$) showed a significant influence of increased SSC rerouting angles on fatty infiltration of the SSC muscle ($P = .008$) (Table 3).

DISCUSSION

Although clinical outcome scores after anterior shoulder stabilization with the Latarjet procedure and ICBGT are comparable,²⁰ this study shows that the described decline

in internal rotation capacity, including range of motion²⁰ and strength,^{7,24} after the Latarjet procedure has a radiographic structural correlate in terms of slight fatty degeneration of the SSC muscle and marked thinning of the tendon at short-term follow-up. As no visual compromise in the ICBGT group was found, our hypothesis was confirmed.

At follow-up, we found that the graft in ICBGT was anatomically remodeled. This process was described in former studies.^{18,19} Even though the Latarjet group showed graft remodeling as previously described,⁹ the inferior aspect of the graft resorbs less due to the pull of the conjoint tendons, leading to an extra-anatomic enlargement of the anteroinferior glenoid rim. In addition, the screws used for graft fixation in the Latarjet procedure stay in place over time and lead to a “metallic enlargement” of the anterior glenoid. Subsequently, in the Latarjet procedure, after horizontal split of the SSC, the upper parts of the musculotendinous unit are rerouted and glide superficially to the graft and screws, which could explain the markedly reduced thickness of the musculotendinous unit at follow-up (Figure 9). Even though technically not measurable in this study, the lower part of the SSC is most likely rerouted inferiorly, which might lead to restriction in rotation (Figure 10).

At follow-up in both groups, none or only mild (grade 1) fatty infiltration of the SSC muscle was seen and muscle diameters were not affected. As described by others,^{21,24} we observed a decreased muscle attenuation in the upper parts of the SSC compared with the lower parts in the Latarjet group, although we noticed no significant differences when comparing the two procedures. Although mean muscle attenuation indicated no decrease in fatty muscle infiltration of SSC muscles, voxel-based quantification showed a significant increase in fatty muscle infiltration of 2% to 5% in the Latarjet group, whereas no differences were seen in ICBGT.

Interestingly, although not significant, an increase in fatty muscle infiltration of the ISP/TM muscle was observed in the Latarjet group. Valencia et al²⁴ investigated SSC integrity after arthroscopic Latarjet procedure and found a

TABLE 2
Measurements for SSC and ISP/TM Structural Muscle Integrity Through SSC Diameters, Mean Muscle Attenuation, and Voxel Quantification^a

	Preoperative			Follow-Up		
	Latarjet	ICBGT	P Value	Latarjet	ICBGT	P Value
SSC diameter, mm						
VD	82.6 ± 10.9	86.3 ± 9.6	.197	82.2 ± 12.0	83.5 ± 9.8	.668
UTD	26.6 ± 3.8	27.3 ± 4.5	.521	26.0 ± 6.0	27.2 ± 4.7	.456
LTD	30.3 ± 5.4	31.0 ± 6.1	.671	28.3 ± 5.2	30.1 ± 5.6	.249
Mean muscle attenuation, HU						
SSC (total)	57.5 ± 5.4	57.4 ± 4.9	.915	56.2 ± 7.6	56.2 ± 7.3	.997
SSC (UMA)	58.1 ± 7.9	59.7 ± 8.8	.510	50.6 ± 9.7	54.7 ± 9.0	.124
SSC (LMA)	59.2 ± 7.4	59.1 ± 5.7	.958	60.7 ± 12.7	58.6 ± 10.9	.515
ISP/TM	66.9 ± 8.5	65.0 ± 9.3	.451	67.6 ± 9.3	66.5 ± 9.1	.651
Fatty muscle infiltration, %						
SSC	2.0 ± 2.9	2.4 ± 2.2	.546	5.3 ± 4.5	2.3 ± 1.7	.001 ^b
ISP/TM	1.7 ± 2.8	2.0 ± 2.5	.630	3 ± 3.6	1.7 ± 1.3	.064

^aValues are expressed as mean ± SD. HU, Hounsfield units; ICBGT, iliac crest bone graft transfer; ISP, infraspinatus; LMA, lower muscle attenuation; LTD, lower transverse diameter; SSC, subscapularis; TM, teres minor; UMA, upper muscle attenuation; UTD, upper transverse diameter; VD, vertical diameter.

^bSignificant difference.

TABLE 3
Linear Regression Model (*R* = 0.447) Investigating the Influence of Postoperative Glenoid Measurements and SSC Rerouting Angles on SSC Fatty Muscle Infiltration^a

	β Coefficient	95% CI		P Value
		Lower Bound	Upper Bound	
Graft area over best-fit circle	-0.177	-0.483	0.129	.251
Graft width over best-fit circle	-0.131	-0.732	0.994	.762
SSC rerouting angle	0.841	0.229	1.454	.008 ^b

^aThe dependent variable was percentage of fatty muscle infiltration of subscapularis (SSC).

^bSignificant correlation.

decrease of internal rotation strength at mid- to long-term follow-up, but ratios to external rotation remained unchanged over the study course. This could be an indicator of concomitant damage to antagonist muscles through impairment of the agonist. Caubère et al⁷ found similar results after short-term follow-up.

Although Edouard et al¹⁰ reported a transient SSC muscle strength weakness and fatigue after Latarjet procedure, Valencia et al²⁴ showed a residual deficit at latest follow-up. In contrast, previously published data²⁰ showed no significant difference of internal or external rotation strength at 2-year follow-up. However, a critical evaluation showed that the measurements were conducted in 0° of arm abduction, neutral rotation, and 90° of elbow flexion, which reflects on functional internal rotation with possible compensation of internal rotators such as the pectoralis muscle, but not merely SSC strength.

In the literature, reduced SSC function after open shoulder stabilization is often attributed to muscle violation upon index surgery, through either tenotomy or split.^{17,21,22} Because surgical approaches in both ICBGT and Latarjet are conducted through a split of the SSC, our results indicate that injuries to the SSC tendon with consecutive compromise of structural muscle integrity are attributed to postoperative mechanical conflict rather than the sole intraoperative trauma. In a recent study, Godenèche et al¹² investigated the effect of screw removal in patients with unexplained anterior shoulder pain after Latarjet procedure and found complete or partial relief of pain, supporting the hypothesis of mechanical conflict between the screw fixation and the SSC.

The strength of the current study is that data were acquired from a prospective randomized controlled trial, and selection bias was therefore minimized. An evaluation of the preoperative state allows for more accurate findings than comparison with the contralateral side. There were 2 main limitations: (1) the follow-up time of 2 years was short, as damage to musculotendinous structures through mechanical friction may progress over time, and (2) although 2 raters completed the measurements with good interobserver reliability, blinding for surgical technique was not possible due to the visible screw fixation on the CT scans. Additionally, patients were placed in the supine position with the arms at the side with no fixed external rotation angle during CT imaging, which could affect the measurements. However, we referenced the measurements to the anatomic features of the scapular body to prevent the influence of varying humeral head translation and rotation. Patients receiving open or arthroscopic Bankart repair before bone augmentation were not excluded from this study. This might also affect the SSC musculotendinous integrity, but as previously reported, there was no

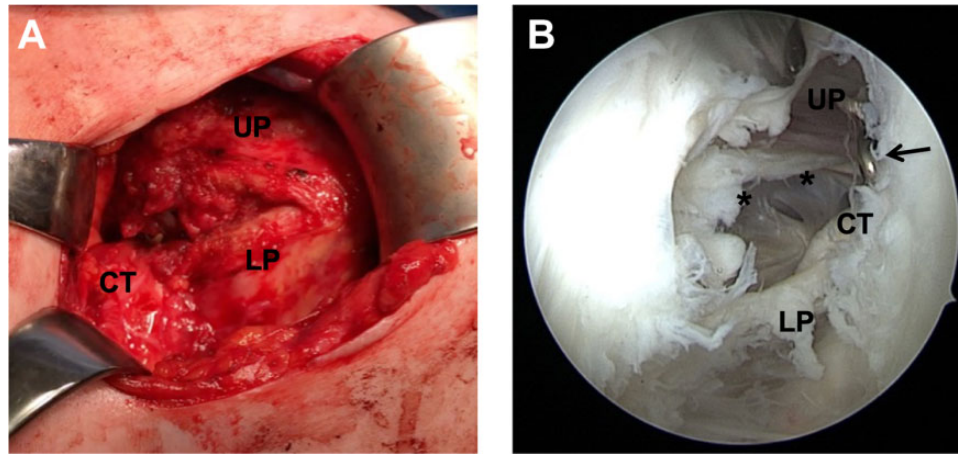


Figure 9. (A) Intraoperative image of permanent horizontal subscapularis (SSC) split after a Latarjet procedure. Upper parts (UP) of the musculotendinous SSC unit protrude over the graft, and lower parts (LP) are redirected underneath the conjoint tendons (CT). (B) Arthroscopic view through an anterolateral viewing portal in a left shoulder that was revised due to persistent anterior shoulder pain after a Latarjet procedure. A marked defect area (asterisks) can be identified in the tendon and muscle of the SSC close to the screw heads (arrow).

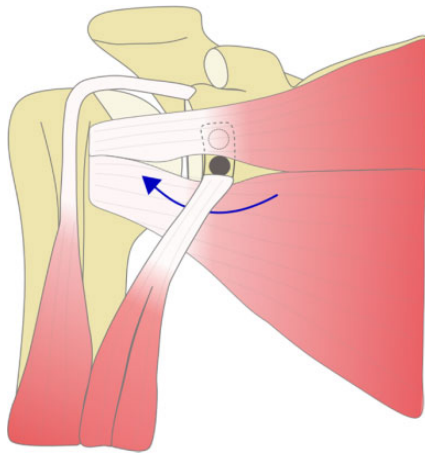


Figure 10. Illustration of subscapularis (SSC) traction force around the coracoid graft in the Latarjet procedure. The upper parts of the SSC are routed over the graft and screw heads, and the lower parts are redirected under the conjoint tendons (blue arrow), which might lead to mechanical conflict.

statistically significant difference in prior procedures in both groups.²⁰

CONCLUSION

Although clinical outcome scores after anterior shoulder stabilization with the Latarjet procedure and ICBGT are comparable, this study shows that the described decline in internal rotation capacity after Latarjet has a radiographic structural correlate in terms of marked thinning and rerouting of the SSC tendon as well as slight fatty degeneration of the muscle. Further studies need to clarify

whether these structural changes might cause long-term problems in individual patients.

REFERENCES

1. Anderl W, Pauzenberger L, Laky B, Kriegleder B, Heuberger PR. Arthroscopic implant-free bone grafting for shoulder instability with glenoid bone loss: clinical and radiological outcome at a minimum 2-year follow-up. *Am J Sports Med.* 2016;44(5):1137-1145.
2. Aubrey J, Esfandiari N, Baracos VE, et al. Measurement of skeletal muscle radiation attenuation and basis of its biological variation. *Acta Physiol (Oxf).* 2014;210(3):489-497.
3. Auffarth A, Schauer J, Matis N, et al. The J-bone graft for anatomical glenoid reconstruction in recurrent posttraumatic anterior shoulder dislocation. *Am J Sports Med.* 2008;36(4):638-647.
4. Baudi P, Righi P, Bolognesi D, et al. How to identify and calculate glenoid bone deficit. *Chir Organi Mov.* 2005;90(2):145-152.
5. Burkhart SS, De Beer JF. Traumatic glenohumeral bone defects and their relationship to failure of arthroscopic Bankart repairs: significance of the inverted-pear glenoid and the humeral engaging Hill-Sachs lesion. *Arthroscopy.* 2000;16(7):677-694.
6. Bushnell BD, Creighton RA, Herring MM. Bony instability of the shoulder. *Arthroscopy.* 2008;24(9):1061-1073.
7. Caubère A, Lami D, Boileau P, et al. Is the subscapularis normal after the open Latarjet procedure? An isokinetic and magnetic resonance imaging evaluation. *J Shoulder Elbow Surg.* 2017;26(10):1775-1781.
8. Chalmers PN, Salazar D, Chamberlain A, Keener JD. Radiographic characterization of the B2 glenoid: is inclusion of the entirety of the scapula necessary? *J Shoulder Elbow Surg.* 2017;26(5):855-860.
9. Di Giacomo G, Costantini A, de Gasperis N, et al. Coracoid graft osteolysis after the Latarjet procedure for anteroinferior shoulder instability: a computed tomography scan study of twenty-six patients. *J Shoulder Elbow Surg.* 2011;20(6):989-995.
10. Edouard P, Bankolé C, Calmels P, Beguin L, Degache F. Isokinetic rotator muscles fatigue in glenohumeral joint instability before and after Latarjet surgery: a pilot prospective study. *Scand J Med Sci Sports.* 2013;23(2):e74-e80.
11. Giles JW, Boons HW, Elkinson I, et al. Does the dynamic sling effect of the Latarjet procedure improve shoulder stability? A biomechanical evaluation. *J Shoulder Elbow Surg.* 2013;22(6):821-827.

12. Godenèche A, Merlini L, Roulet S, et al. Screw removal can resolve unexplained anterior pain without recurrence of shoulder instability after open Latarjet procedures. *Am J Sports Med.* 2020;48(6):1450-1455.
13. Goutallier D, Postel JM, Bernageau J, Lavau L, Voisin MC. Fatty muscle degeneration in cuff ruptures: pre- and postoperative evaluation by CT scan. *Clin Orthop Relat Res.* 1994;304:78-83.
14. Lafosse L, Boyle S. Arthroscopic Latarjet procedure. *J Shoulder Elbow Surg.* 2010;19(2)(suppl):2-12.
15. Landis JR, Koch GG. The measurement of observer agreement for categorical data. *Biometrics.* 1977;33(1):159-174.
16. Latarjet M. Treatment of recurrent dislocation of the shoulder [in French]. *Lyon Chir.* 1954;49(8):994-997.
17. Maynou C, Cassagnaud X, Mestdagh H. Function of subscapularis after surgical treatment for recurrent instability of the shoulder using a bone-block procedure. *J Bone Joint Surg Br.* 2005;87(8):1096-1101.
18. Moroder P, Hirzinger C, Lederer S, et al. Restoration of anterior glenoid bone defects in posttraumatic recurrent anterior shoulder instability using the J-bone graft shows anatomic graft remodeling. *Am J Sports Med.* 2012;40(7):1544-1550.
19. Moroder P, Hitzl W, Tauber M, et al. Effect of anatomic bone grafting in post-traumatic recurrent anterior shoulder instability on glenoid morphology. *J Shoulder Elbow Surg.* 2013;22(11):1522-1529.
20. Moroder P, Schulz E, Wierer G, et al. Neer Award 2019: Latarjet procedure vs. iliac crest bone graft transfer for treatment of anterior shoulder instability with glenoid bone loss: a prospective randomized trial. *J Shoulder Elbow Surg.* 2019;28(7):1298-1307.
21. Scheibel M, Nikulka C, Dick A, et al. Structural integrity and clinical function of the subscapularis musculotendinous unit after arthroscopic and open shoulder stabilization. *Am J Sports Med.* 2007;35(7):1153-1161.
22. Scheibel M, Tsynman A, Magosch P, Schroeder RJ, Habermeyer P. Postoperative subscapularis muscle insufficiency after primary and revision open shoulder stabilization. *Am J Sports Med.* 2006;34(10):1586-1593.
23. Schneider CA, Rasband WS, Eliceiri KW. NIH Image to ImageJ: 25 years of image analysis. *Nat Methods.* 2012;9(7):671-675.
24. Valencia M, Fernandez-Bermejo G, Martin-Rios MD, et al. Subscapularis structural integrity and function after arthroscopic Latarjet procedure at a minimum 2-year follow-up. *J Shoulder Elbow Surg.* 2020;29(1):104-112.
25. Warner JJ, Gill TJ, O'Hollerhan JD, Pathare N, Millett PJ. Anatomical glenoid reconstruction for recurrent anterior glenohumeral instability with glenoid deficiency using an autogenous tricortical iliac crest bone graft. *Am J Sports Med.* 2006;34(2):205-212.
26. Zanetti M, Gerber C, Hodler J. Quantitative assessment of the muscles of the rotator cuff with magnetic resonance imaging. *Invest Radiol.* 1998;33(3):163-170.